Rapid oxygen utilization in the ocean twilight zone assessed with the cosmogenic isotope ^{7}Be

David Kadko[1]

Received 9 March 2009; revised 30 June 2009; accepted 17 July 2009; published 21 October 2009.

[1] The rate of oxygen utilization beneath the sunlit surface ocean provides a measure of the export rate of biologically produced carbon to the deep sea, and its variation with depth suggests where remineralization of that carbon occurs. The latter consideration is relevant to the efficiency of carbon sequestration in deep water. However, accurate characterization of this process, particularly within 200 m of the euphotic zone where carbon utilization is most intense, has been difficult owing to limitations of techniques applied to these shallow depths. Here, a novel approach utilizing the cosmogenic isotope ^{7}Be indicates that at a site in the subtropical North Atlantic, 65% of sinking carbon is remineralized within 200 m of the ocean's surface and is thus readily available for return to the atmosphere. The corresponding oxygen utilization rates are greater than would be suggested by the attenuation with depth of organic matter measured by shallow sediment traps.

Citation: Kadko, D. (2009), Rapid oxygen utilization in the ocean twilight zone assessed with the cosmogenic isotope ^{7}Be, *Global Biogeochem. Cycles*, *23*, GB4010, doi:10.1029/2009GB003510.

1. Introduction

[2] The downward flux of biologically produced particulate carbon from the ocean's euphotic zone is significant to the global carbon cycle, climate, and deep sea ecology. While the majority of this material is respired before reaching the seafloor, the functionality of remineralization with depth controls the time scale over which carbon can be sequestered before return to the atmosphere and affects the distribution of nutrition within the aphotic ecosystem. If sinking particulate organic carbon (POC) persists to depths greater than wintertime mixed layers (hundreds of meters) then the period of sequestration will be comparable to deep ocean circulation times of hundreds of years. However shallower remineralization suggests that this carbon would be exposed to the atmosphere within a time scale of only several years or less [*Martin et al.*, 1987, 1993]. The efficiency of organisms in metabolizing this material as it settles out of the euphotic zone ultimately controls its distribution within the water column.

[3] POC fluxes measured with sediment traps show a sharp decline with depth in the upper 200 m of the ocean "twilight zone," which is the dimly lit portion of the water column beneath the euphotic zone from ~100 m extending to 1000 m depth [*Martin et al.*, 1987, 1993; *Buesseler et al.*, 2007; *Lampitt et al.*, 2008; *Berelson*, 2001]. Exact quantification of the depth-dependent POC flux via this approach has been difficult because of uncertainties in the trapping efficiency, despite recent advances in sediment trap technology [*Buesseler et al.*, 2007; *Lampitt et al.*, 2008]. As respiration will leave an imprint on ocean chemistry, it is possible to compare the trap-determined attenuation of POC to other estimates of organic carbon remineralization. For example, the rapid remineralization of POC implied by shallow sediment trap observations should be manifested by high oxygen utilization rates (OUR) below the euphotic zone. This quantity has been estimated by several approaches aimed to derive the carbon export flux by vertical integration of OUR. However, accurate characterization of OUR, particularly within 200 m of the euphotic zone where carbon utilization is most intense, has been difficult owing to limitations of techniques applied to these shallow depths. Significant differences among these methods are found, arising at least in part from the different time scales of the various approaches. For example, in vitro determination of respiration rates between 100 and 200 m in the North Pacific [*Williams and Purdie*, 1991] yielded values that are much higher than OUR implied by the decline of POC observed in most trap studies (Figure 1). These values, which can be considered "instantaneous" measures of OUR, were also substantially greater than OUR estimated by tracer-based time estimates applied to measurements of apparent oxygen utilization (AOU). The tracers commonly used in these studies, such as the ^{3}H-^{3}He couple and chlorofluorocarbons [e.g., *Jenkins*, 1977, 1998; *Jenkins and Wallace*, 1992] are characterized by multiyear to decadal time scales and likely miss the rapid organic matter remineralization occurring along shallow isopycnal surfaces.

[4] To estimate OUR within the shallow water just beneath the euphotic zone, where the most significant remineralization is occurring, a time tracer appropriate for

[1]Division of Marine and Atmospheric Chemistry, Rosenstiel School of Marine and Atmospheric Science, University of Miami, Miami, Florida, USA.

0886-6236/09/2009GB003510$12.00

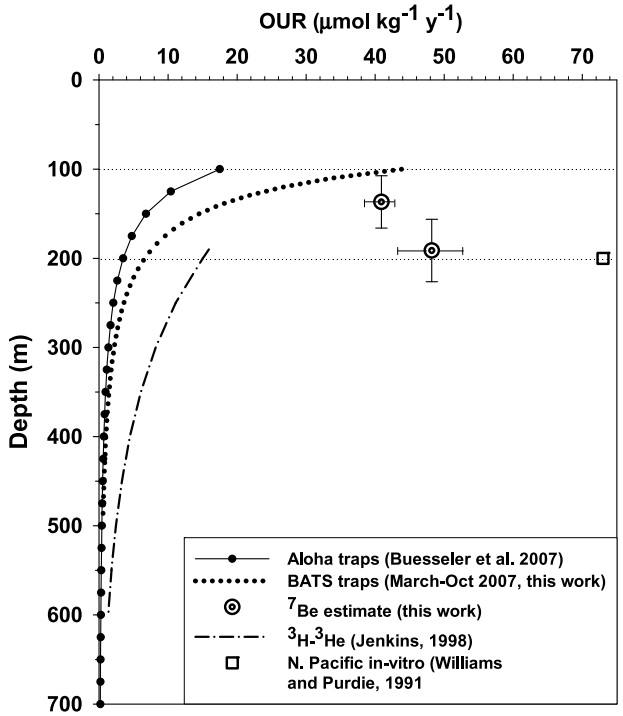

Figure 1. Oxygen utilization rate (OUR) profiles obtained by several methods for the Sargasso Sea and North Pacific. The particulate organic carbon (POC) flux (F) reported for the ALOHA traps (22°45′N, 158°W) and the Bermuda Atlantic Time-series Study (BATS) were converted to the OUR profile using equation (5). The ALOHA trap rates are substantially less than those derived from a composite of in vitro measurements in the same general area (~28.5°N, 154.50°W). At BATS, the integrated OUR implied by the trap flux between 100–200 m is only 40% of that derived from the ^{7}Be tracer technique. The shallow ^{7}Be-derived value neglects oxygen production and is thus a conservative calculation. The OUR profile estimated from the ^{3}H-^{3}He technique in the subtropical North Atlantic is also indicated.

seasonal time scales is needed. Here ^{7}Be, a cosmic ray produced radioactive nuclide with a half-life of 53.3 days, is utilized for this purpose. As discussed below, the oxygen utilization rates derived by this method are greater than would be suggested by the attenuation with depth of organic matter measured by shallow sediment traps. Samples for this study were collected monthly, from June to November 2007, in the vicinity of the US JGOFS Bermuda Atlantic Time-series Study (BATS, 31°40′N, 64°10′W) and Hydrostation S (32°10′N, 64°30′W) in the Sargasso Sea.*

2. Background: ^{7}Be

[5] Be-7 is deposited upon the ocean surface by rainfall and subsequently homogenized within the surface mixed layer [*Silker*, 1972; *Aaboe et al.*, 1981; *Young and Silker*, 1980; *Kadko and Olson*, 1996; *Kadko*, 2000]. Over broad oceanic regions, the ^{7}Be inventory varies as a function of rainfall, and therefore mixed layer concentrations are inversely related to salinity [*Young and Silker*, 1980; *Kadko and Olson*, 1996]. On smaller scales, for a given input of ^{7}Be, the mixed layer depth (MLD) is a critical parameter that largely determines the ^{7}Be surface activity, and as the North Atlantic MLD varies seasonally in a fairly regular way, the ^{7}Be activity likewise will vary in a predictable fashion in this region over the course of a year (Figures 2a and 2b) [*Kadko and Olson*, 1996]. Therefore the major features of oceanic ^{7}Be profiles can be generated by a simple model that accounts for the seasonal deepening and shoaling of the mixed layer on the basis of empirical observations of the mixed layer history [*Kadko and Olson*, 1996; *Kadko*, 2000]. In the spring, when the mixed layer is at its deepest, the ^{7}Be, input over the previous season, is uniformly distributed through the deep mixed layer. Thereafter, upon restratification, the mixed layer shoals and the ^{7}Be activity in the shoaling mixed layer increases as the input flux is distributed over a smaller volume. The remnant ^{7}Be beneath the mixed layer decays radioactively as this water is now isolated from further atmospheric input (Figures 2b and 2c). Similarly, O_2 beneath the mixed layer is no longer affected by gas exchange, and below the euphotic zone will be utilized during respiration of organic matter (Figure 2d). By comparing the decrease of oxygen to the decay of ^{7}Be it is possible to derive the rate of oxygen utilization beneath the mixed layer. The June–November time frame of this study captures the period of restratification after maximum MLD in the spring to the initial mixed layer deepening in late fall.

[6] To apply this technique, a modification of an approach that employs radium−228 to derive OUR is used [*Sarmiento et al.*, 1990]. For oxygen, a measure of aging (τ_{O2}) of a water parcel along an isopycnal is represented by

$$\tau_{O2} = (\mathrm{AOU}_{\tau} - \mathrm{AOU}_{i})/\mathrm{OUR} \quad (1a)$$

where

AOU_{τ} = apparent oxygen utilization measured in the water column at time τ (μmol kg^{-1}).

AOU_{i} = apparent oxygen utilization measured in the water column at some initial time.

[7] Note that in this formulation, $\mathrm{AOU_i}$ need not be the surface concentration which usually is taken as zero (i.e., the O_2 is assumed to be in equilibrium with the atmosphere). This precludes assuming that the surface waters are in a state of saturation and focuses on the gradient of AOU with time.

[8] In shallow layers beneath the mixed layer, primary production may not be zero. This equation could then be expressed as

$$\tau_{O2} = (\mathrm{AOU}_{\tau} - \mathrm{AOU}_{i})/\mathrm{OUR}^{*} \quad (1b)$$

OUR* is an apparent oxygen utilization rate which equals (OUR − p) where p is primary production. In the discussion that follows, the OUR term is retained but with the understanding that in certain instances represents a lower limit due to oxygen production.

*The sentence is correct here. The article as originally published appears online.

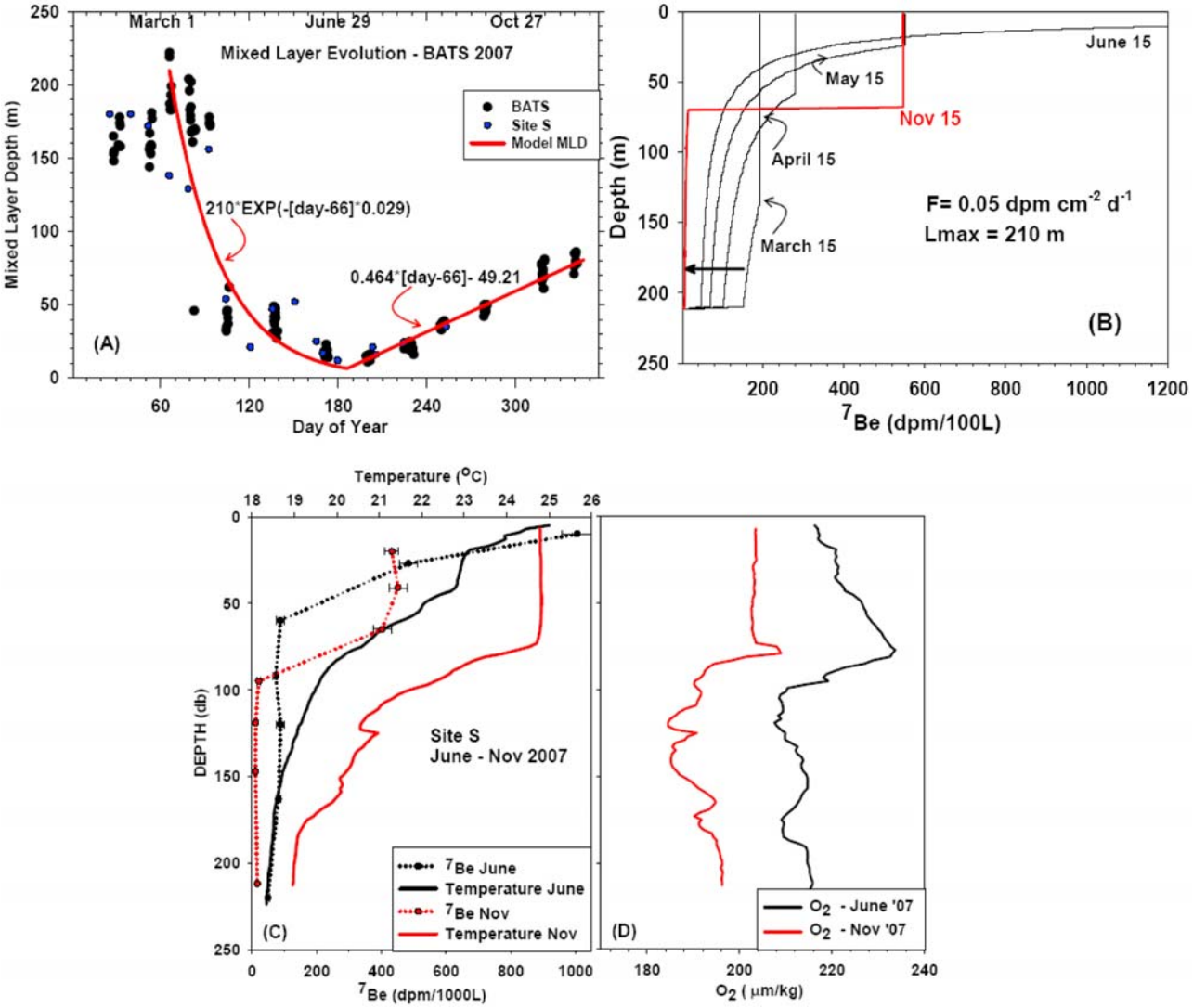

Figure 2. (a) Seasonal evolution of the mixed layer depth (MLD) for the study area in 2007 (dark circles are observations). Mathematical representations of the trends used in the model are shown. (b) Results from the simple one-dimensional model illustrating how, with the measured flux of ^{7}Be (F) and the known MLD history (L_{max} is the maximum MLD), month-to-month profiles of ^{7}Be can be generated in response to the evolving mixed layer depth. The arrow indicates the decay of ^{7}Be beneath the mixed layer after the onset of restratification. (c) Observed temperature and ^{7}Be profiles for June and November 2007 at Hydrostation S indicating that the model captures the major features of the ^{7}Be data. (d) The corresponding profiles of oxygen concentration showing the decrease from June to November.

[9] For the same initial and observation times, a measure of aging utilizing ^{7}Be can be formulated:

$$\tau_{7\mathrm{Be}} = \left[\ln\left({}^{7}\mathrm{Be}_i/{}^{7}\mathrm{Be}_\tau\right)\right]/\lambda_{7\mathrm{Be}} \qquad (2)$$

For the identical water mass, $\tau_{O2} = \tau_{7\mathrm{Be}}$, and

$${}^{7}\mathrm{Be}_\tau = {}^{7}\,\mathrm{Be}_i \exp[-\lambda(\mathrm{AOU}\tau - \mathrm{AOU}_i)/\mathrm{OUR}] \qquad (3)$$

In an analysis of the ^{3}H-^{3}He tracer to assess OUR, it was noted that age-AOU relationships on shallow isopycnals are not significantly impacted by mixing [*Jenkins*, 1998], and therefore over the relatively short half life of ^{7}Be it is reasonable to expect that the advective assumption implicit in this approach is valid. For example, with a vertical diffusivity (K_z) of 1×10^{-5} m^2/s, the diffusional transport length over the 77-day mean life (T) of ^{7}Be is $\sqrt{(K_z \times T)}$ or $\sim$8 m, which is small compared to the range of isopycnal depths considered in this study (described in section 4).

[10] Another assumption is that the OUR is constant throughout the period of observation. Exported DOC into the mesopelagic generally reaches seasonal background values after the spring bloom by June–July [*Hansell and Carlson*, 2001], which implies a relatively constant rate of remineralization. However, individual production events,

Table 1. The ^{7}Be Extraction Efficiencies

Volume (L)	Extraction Efficiencies
300	0.839 ± 0.034
400	0.819 ± 0.028
500	0.805 ± 0.029
600	0.782 ± 0.024
700	0.757 ± 0.023

for example, those triggered by ubiquitous eddies in this region, [*McGillicuddy et al.*, 1998; *Oschlies and Garcon*, 1998] could lead to short-term variability of OUR over the observational period.

[11] Finally, there is an implicit assumption of constant initial ^{7}Be and O_2 concentration in this approach. The extent to which source waters extend over broad regional gradients in rainfall would affect the input of ^{7}Be, and this would be reflected in variable salinity. Within the isopycnals studied (discussed in section 4) there is only a small range of salinity which implies a relatively constant input of ^{7}Be. Variability in the mixed layer depth, however, particularly in the early spring (Figure 2a) could contribute to variability in initial concentrations. Interannual variability of ^{7}Be flux is not problematic to the application here as the tracer is relevant to only the seasonal time scale.

3. Methods

[12] Vertical profiles of ^{7}Be were collected in the NE Atlantic during June–November 2007 from the R/V *Atlantic Explorer*. The methods are slightly modified from an earlier work [*Kadko and Olson*, 1996]. Beryllium-7 was collected by pumping 400–700 L of seawater through iron-impregnated acrylic fibers [*Lal et al.*, 1988; *Krishnaswami et al.*, 1972; *Lee et al.*, 1991] packed in cylindrical cartridges. The water was taken at various depths through a 1.5-inch hose whose end was attached to a conductivity-temperature-depth system. The pumping was achieved with a deck-mounted centrifugal pump at a rate of ~12 L/min. The efficiency of the fiber for extraction of Be from seawater was determined by adding 500 mL of a 1000 ppm Be atomic absorption standard to a drum containing seawater. The seawater was pumped through an iron fiber cartridge, and at every 100 L the Be content of the cartridge effluent was measured by atomic absorption. From this data, the integrated Be extraction efficiencies were calculated. Six such trials were performed on fibers made from three different fiber batches. The average extraction efficiencies are shown in Table 1. On land, the fibers were dried and then ashed. The ash was subsequently pressed into a pellet (5.8-cm diameter) and placed on a low background germanium gamma detector. In some cases, two fibers were taken from the same depth (typically greater than 190 m) to assure adequate signal and combined, ashed, and placed in a Marinelli beaker configuration. For such samples, up to ~1200 L were analyzed.

[13] The ^{7}Be has a readily identifiable gamma peak at 478 keV. The detector was calibrated for the pellet and Marenelli beaker geometries by adding a commercially prepared mixed solution of known gamma activities to an ashed fiber, pressing the ash into a pellet or adding the ash to a beaker, and counting the activities to derive a calibration curve. The counting efficiencies were adjusted to the height of the pellets (ranging from 9–12 mm) by preparing pellet standards of different heights. Similarly, the Marenelli beakers were calibrated for different ash weights. The error for each measurement is the statistical counting error (δ) and the uncertainty in the blank, $\sqrt{(\delta^2 + \delta_b^2)}$, multiplied by

$$[(\lambda \times \mathrm{CT})/(1 - \exp(-\lambda \times \mathrm{CT}))] \times [\exp(\lambda \times D)/(\mathrm{CE} \times \mathrm{FE} \times \mathrm{PE})]$$

where D is the number of days after sample collection, λ is the decay constant (0.013 d^{-1}), CT is the counting time, CE is the counting efficiency of the 478 keV gamma, FE is the fiber extraction efficiency, and PE is the photon emission fraction (0.104) for ^{7}Be. The uncertainties of the extraction efficiency (4%) and the detector efficiency (2%) were in all cases smaller than the statistical counting error and the uncertainty in the blank.

4. Results and Discussion

[14] The sample data are presented in Table 2. For this study, profiles taken within eddies (determined through satellite-derived sea level anomaly data) were excluded so as to avoid potential variability in ^{7}Be and O_2 source function. In addition, samples were evaluated for primary production through the BATS online database (ftp://ftp.bios.edu/BATS/bottle/bats_production.txt) to ensure that those influenced by significant O_2 production were not used. Generally, production drops off rapidly at depths greater than 80 m and by 140 m is ~1% of the maximum euphotic zone values. Several points shallower than 120 m were eliminated where the online data suggested significant (>10% of maximum euphotic zone value) productivity. Oxygen production not accounted for would lead to an underestimate of OUR (see equation (1b)).

[15] In Figure 3, ^{7}Be is plotted against AOU for two potential density surfaces beneath the mixed layer (σ_θ = 26.0–26.29, corresponding to an average depth of 136.7 ± 29.4 m, and σ_θ = 26.3–26.43, corresponding to an average depth of 191.2 ± 35.0 m). Data were taken over the 6-month period June–November 2007. The plots show the expected month-to-month decrease of ^{7}Be with increasing AOU as organic carbon is respired. Within the density range 26.0–26.29, the best fit solution (R^2 = 0.91) for equation (3) indicates an OUR = 0.112 μmol $kg^{-1}d^{-1}$. The model fit, along with the 1σ and 2σ uncertainty curves, is shown in Figure 3a. This result is conservative as it neglects the small oxygen production remaining at this isopycnal depth range, but likely underestimates OUR by no more than 30%. For the density range 26.3–26.43 the best fit solution (R^2 = 0.70) yields an OUR = 0.132 μmol $kg^{-1}d^{-1}$ (curves plotted in Figure 3b). Sources of uncertainty in these results may include variability in the initial ^{7}Be and O_2 concentrations discussed earlier, as well as factors that cause departures from the one-dimensional model described in Figure 2. For example, despite the effort to avoid eddies, some stations were taken near eddies which likely influenced the observed profiles. In addition, intrusions of layers, such as 18 degree

Table 2. The 2007 Sample Data

Station	Depth	Salinity	Temperature (°C)	σ_θ	^{7}Be (dpm/1000 L)	AOU (μmol/kg)
			June			
Site 'S'	163	36.62	18.51	26.38	81.78 ± 6.30	16.06
	220	36.60	18.30	26.43	48.47 ± 5.10	15.40
BATS	150	36.66	19.23	26.23	67.14 ± 5.57	12.00
	210	36.64	18.88	26.31	59.44 ± 4.93	15.10
SE BATS[a]	150	36.65	18.96	26.29	78.10 ± 5.37	13.25
	210	36.61	18.48	26.38	35.16 ± 4.03	20.83
			July			
Site 'S'	93	36.66	19.10	26.26	39.17 ± 13.26	17.26
	128	36.62	18.75	26.33	4.05 ± 3.02	25.15
	199	36.61	18.30	26.43	24.18 ± 8.44	19.42
BATS	90	36.66	19.40	26.19	51.50 ± 11.59	15.60
	120	36.64	18.80	26.33	49.35 ± 10.22	19.00
	157	36.61	18.42	26.40	37.48 ± 6.32	23.11
	215	36.60	18.25	26.44	44.43 ± 5.36	16.87
			August			
Site 'S'	122	36.67	19.31	26.22	28.45 ± 9.36	10.57
	156	36.62	18.67	26.35	4.05 ± 3.02	23.80
	209	36.58	18.28	26.41	24.89 ± 7.81	24.41
BATS	124	36.65	19.07	26.27	28.31 ± 9.19	18.65
	150	36.63	18.79	26.33	39.97 ± 3.63	22.56
	209	36.59	18.38	26.40	18.80 ± 7.90	26.70
			September			
Site 'S'	118	36.68	19.77	26.11	26.84 ± 11.91	22.90
	151	36.67	19.20	26.25	14.64 ± 6.97	24.90
	228	36.62	18.44	26.40	15.88 ± 5.38	25.35
			October			
BATS	118	36.70	20.13	26.02	25.89 ± 10.85	24.18
	154	36.70	19.23	26.24	8.41 ± 7.39	27.14
	219	36.63	18.59	26.38	22.96 ± 4.73	27.00
Station 11[b]	153	36.67	19.24	26.24	10.19 ± 6.61	25.44
	221	36.60	18.44	26.39	19.20 ± 7.20	28.56
			November			
Site 'S'	147	36.70	20.23	26.00	10.54 ± 2.48	35.65
	212	36.64	18.97	26.29	16.20 ± 2.73	31.04
BATS	125	36.715	20.22	26.01	20.31 ± 4.12	21.78
	159	36.66	19.33	26.21	9.02 ± 3.65	30.36
	216	36.61	18.59	26.36	23.14 ± 3.40	27.70

[a]31°25′N, 63°46′W.
[b]31°12′N, 64°17′W.

mode water [*Kadko and Johnson*, 2008], were evident in some profiles. Such effects would likely be more acute in the deeper isopycnals than in the more recently ventilated shallow water.

[16] The results are shown in Figure 1 with other estimates of OUR for the Sargasso Sea and the North Pacific. The depth-integrated average OUR derived from ^{7}Be (100–200 m) is 4.46 ± 0.39 (1σ) mol O_2 m^{-2}yr^{-1}. This is somewhat higher than the 3.0–3.5 mol m^{-2}yr^{-1} derived from oxygen stock assessment within 100–250 m for the BATS site between 1992 and 1998 [*Hansell and Carlson*, 2001]. Combining the ^{7}Be-derived value (integrated between 100 and 200 m) with the estimate based on ^{3}H-^{3}He [*Jenkins*, 1998] (integrated between 200 and 1000 m), total oxygen consumption is 6.9 mol O_2 m^{-2}yr^{-1}. With a stoichiometric conversion factor for ΔO_2:ΔC of 1.4:1, this equates to a carbon respiration rate of 4.9 mol C m^{-2}yr^{-1}, a value comparable to the 5.6 mol C m^{-2}yr^{-1} new production rate derived independently for the Sargasso Sea using the ^{3}He flux gauge technique, which is based on the observed correlation of ^{3}He to nitrate in the regional upper thermocline [*Jenkins and Doney*, 2003].

[17] The ^{7}Be estimate of carbon respiration can also be compared to that derived from the attenuation with depth of POC measured by shallow sediment traps over the period of ^{7}Be sampling. The POC accumulation rate from the BATS traps at 150, 200, and 300 m, averaged over April–November 2007 (http://bats.bios.edu/bats_form_trap.html), were used to derive a POC flux profile using the equation of *Martin et al.* [1993]. April was chosen as the starting point so as to capture the effect of C input within a mean life of the initial ^{7}Be sampling in June. The Martin equation describes the POC flux (F) as a function of depth z:

$$F = F_{150}(z/150)^{-b} \tag{4}$$

where F_{150} is the observed flux at 150 m and b is a parameter that determines the depth-dependent flux attenuation. A value of $b = 1.73$ is used for the BATS data (Figure 4). Then, the POC flux (F) was converted to the OUR profile using the approach from *Martin et al.* [1993]:

$$\mathrm{OUR} = 1.4(F_{150}b/150)(z/150)^{-b-1} \tag{5}$$

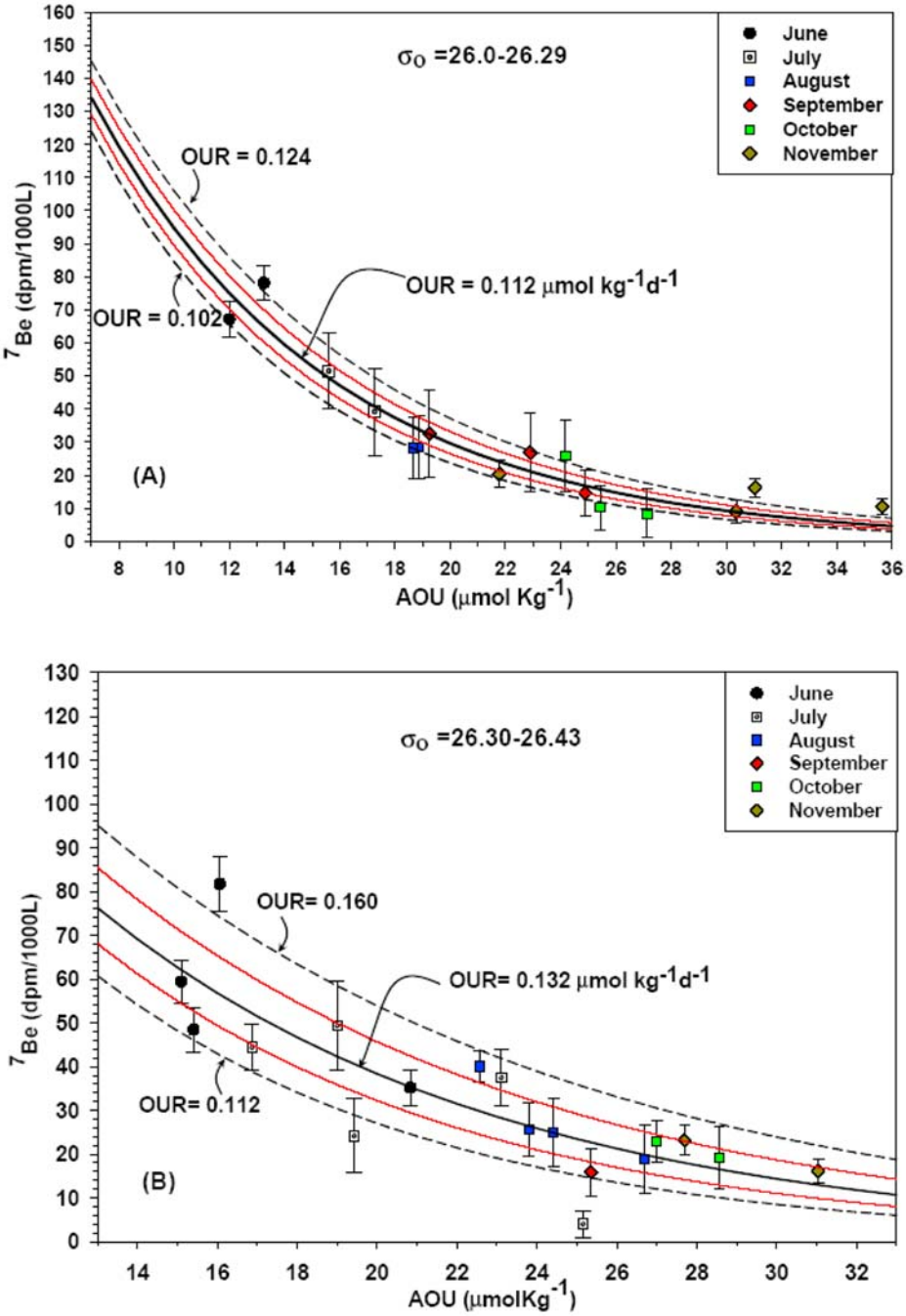

Figure 3. Be-7 plotted against AOU over the period June–November 2007 for (a) the density range σ_θ = 26.0–26.29, where the best fit (R^2 = 0.91) model curve for equation (3) (solid black line) yields an OUR = 0.112 μmol kg^{-1}d^{-1} and (b) the density range σ_θ = 26.3–26.43, where the best fit (R^2 = 0.70) model curve for equation (3) (solid black line) yields an OUR = 0.132 μmol kg^{-1}d^{-1}. For each density range, monthly samples are indicated by symbols. The 1σ (red lines) and 2σ uncertainty (dashed, labeled black lines) curves are shown.

where 1.4 is the stoichiometric ΔO_2:ΔC conversion factor (Figure 1).

[18] Within the 100–200 m depth zone, carbon respiration based on the attenuation with depth of POC measured by shallow sediment traps over the period of ^{7}Be sampling is only 1.3 mol C m^{-2}y^{-1}, while that based on ^{7}Be is 3.19 mol C m^{-2}yr^{-1}. Similarly, the integrated 100–1000 m estimate from the combined ^{7}Be and ^{3}H–^{3}He methods of 4.9 mol C m^{-2}yr^{-1} is considerably larger than the 1.8 mol C m^{-2}yr^{-1} suggested by the trap data (Figure 1).

[19] Several factors can lead to a mismatch between respiration based on OUR and that which is implied by

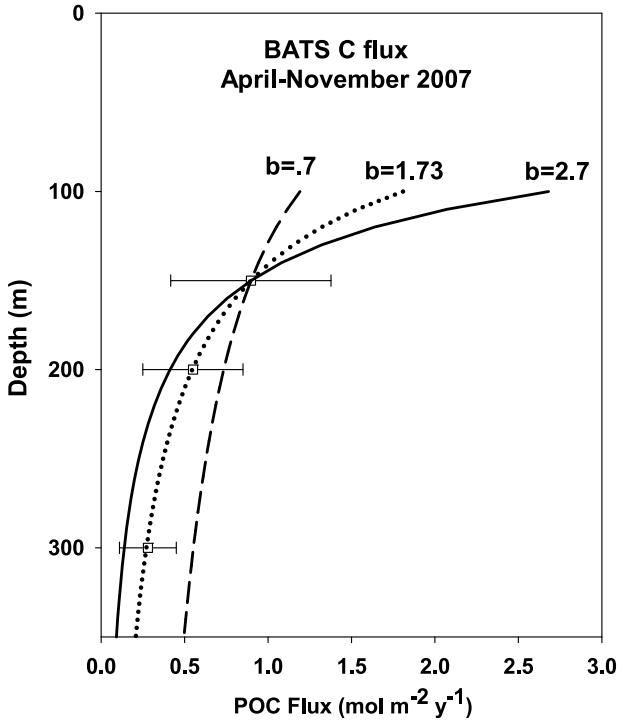

Figure 4. The POC accumulation rate from the BATS traps at 150, 200, and 300 m, averaged over April–November 2007. Several fits to the Martin equation (equation (4)) are presented.

the vertical attenuation of POC, all of which lend to the trap results being a lower limit of downward organic carbon flux. These include vertical migration of zooplankton, export and respiration of DOC, missed episodic events, lateral input of POC, trap collection inefficiency, and chemoautotrophy. The OUR effectively includes and integrates these effects that would not readily be captured by sediment traps. Some of these processes can be evaluated. A study of zooplankton vertical migration at the BATS site indicated that on an annual basis this contribution was relatively minor, accounting for a carbon flux of 0.06 mol C $m^{-2}yr^{-1}$ [*Steinberg et al.*, 2000]. It has been reported that exported DOC oxidation drove 24–64% of the annual oxygen utilization rate in the 100–250 m depth range at BATS between 1992 and 1998 [*Hansell and Carlson*, 2001]. Observations made during the present study for the 26.0–26.29 density surface indicate that 18% of the AOU can be accounted for by DOC oxidation (Figure 5a). For the deeper density region, 26% of the AOU can be accounted for by DOC respiration but the correlation was poor (Figure 5b). This result might indicate that deeper semilabile DOC is more recalcitrant than that of shallower layers [*Carlson*, 2002]. Allowing that ~20% of the OUR between 100–200 m is driven by DOC, then 0.2 × 3.19 mol C $m^{-2}yr^{-1}$ or ~0.6 mol C $m^{-2}yr^{-1}$ can be accounted for. This is within the 0.4–1.4 mol C $m^{-2}yr^{-1}$ range of DOC export flux at BATS reported for the period 1992–1998 [*Hansell and Carlson*, 2001; *Carlson et al.*, 1994]. At BATS, it appears that vertical migration and DOC fluxes are insufficient to completely cover the OUR-POC flux mismatch. It has been suggested that episodic events driven by eddy-induced nutrient injection might contribute to this balance [*McGillicuddy et al.*, 1998; *Oschlies and Garcon*, 1998]. Also, lateral transport of suspended POC (undersampled by traps) might be responsible for a significant portion of the excess oxygen consumption rates relative to the sinking POC and DOC supply [*Baltar et al.*, 2009; *Aristegui et al.*, 2005].

5. Conclusions

[20] Within the ocean twilight zone, significant oxygen consumption occurs through biological respiration of organic carbon delivered from the surface ocean. Differences

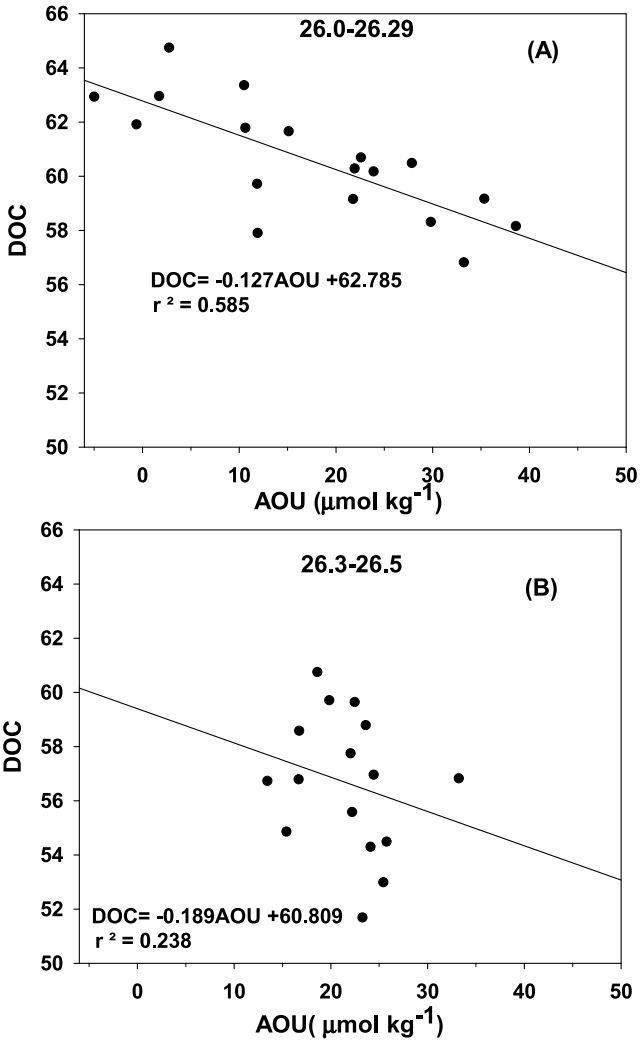

Figure 5. (a) DOC plotted against AOU for the density range 26.0–26.29. The slope of the line is ~18% of that expected (using a respiration quotient, C/O_2, of 0.72) were all the increase in AOU due to respiration of DOC. (b) DOC plotted against AOU for the density range 26.3–26.5. The slope of the line is ~26% of that expected were all the increase in AOU due to respiration of DOC, but a strong correlation is not observed.

in estimates obtained by various methods arise at least in part from the different time scales over which these techniques can be applied. In essence, OUR is a time-dependent variable that decreases as observational time scales increase. This relates to pools of organic carbon characterized by different degrees of reactivity such that more labile carbon is respired immediately below the euphotic zone, and more refractory components persist to greater depths [*Martin et al.*, 1993; *Carlson*, 2002; *Carlson et al.*, 1994; *Clegg and Whitfield*, 1990; *Kirchman et al.*, 1993] The time required for seasonally exported DOC to remineralize within 100–250 m at BATS was reported as 40 to 98 days [*Hansell and Carlson*, 2001] suggesting that the seasonal time scale of the ^{7}Be tracer technique allows it to capture that portion of shallow OUR derived from rapid DOC consumption, and, by inference, rapid consumption of highly labile POC freshly delivered from the euphotic zone. This is significant, as the rates derived here are appreciably greater than those suggested by sediment traps and indicate that 65% of sinking carbon within the twilight zone is remineralized within 200 m of the ocean's surface and thus readily available for return to the atmosphere. This is relevant to the efficacy of geoengineering approaches such as iron-fertilization to sequester carbon to abyssal depths [*Boyd et al.*, 2007].

[21] Carbon sequestration in the deep sea is an essential element for modeling the fate of enhanced carbon input into the atmosphere, requiring depth-dependent parameterization of the transport and remineralization of organic carbon. Oxygen utilization rates provide an integrated assessment of the processes and distribution of carbon respiration over a large range of temporal and spatial scales. Development of tracer techniques and observing technologies [e.g., *Martz et al.*, 2008] applied over appropriate time scales will improve basin-scale estimates of the magnitude of this quantity and the assessment of the export flux of carbon from the surface ocean and its feedback on atmospheric CO_2 and climate.

[22] **Acknowledgments.** The author wishes to thank the captain and crew of R/V *Atlantic Explorer* for their able field support. Mark Stephens provided important at-sea and laboratory technical assistance. Field assistance from, and scientific discussions with, Rod Johnson were instrumental in bringing this work to fruition. Discussions with Dennis Hansell, Steve Emerson, and Paul Quay were greatly appreciated. Comments by two anonymous reviewers were very helpful. This work was supported by the Chemical Oceanography Program of the NSF, grant OCE-0549522.

References

Aaboe, E., E. P. Dion, and K. K. Turekian (1981), ^{7}Be in Sargasso Sea and Long Island Sound waters, *J. Geophys. Res.*, *86*, 3255–3257, doi:10.1029/JC086iC04p03255.

Aristegui, J., C. M. Duarte, J. M. Gasol, and L. Alonso-Sáez (2005), Active mesopelagic prokaryotes support high respiration in the subtropical northeast Atlantic Ocean, *Geophys. Res. Lett.*, *32*, L03608, doi:10.1029/2004GL021863.

Baltar, F., J. Aristegui, J. M. Gasol, E. Sintes, and G. J. Herndl (2009), Evidence for dependence of prokaryotic metabolism on suspended particulate organic matter in the dark waters of the subtropical North Atlantic, *Limnol. Oceanogr.*, *54*, 182–193.

Berelson, W. M. (2001), The flux of particulate organic carbon into the ocean interior: A comparison of four U.S. JGOFS Regional Studies, *Oceanography*, *14*, 59–67.

Boyd, P. W., et al. (2007), Mesoscale iron enrichment experiments 1993–2005: Synthesis and future directions, *Science*, *315*, 612–617, doi:10.1126/science.1131669.

Buesseler, K. O., et al. (2007), Revisiting carbon flux through the ocean's twilight zone, *Science*, *316*, 567–570, doi:10.1126/science.1137959.

Carlson, C. A. (2002), Production and consumption processes, in *Biogeochemistry of Marine Dissolved Organic Matter*, edited by D. A. Hansell and C. A. Carlson, pp. 91–151, Academic Press, San Diego, Calif.

Carlson, C. A., H. W. Ducklow, and A. F. Michaels (1994), Annual flux of dissolved organic carbon from the euphotic zone in the northwestern Sargasso Sea, *Nature*, *371*, 405–408, doi:10.1038/371405a0.

Clegg, S. L., and M. Whitfield (1990), A generalized model for the scavenging of trace metals in the open ocean: I. Particle cycling, *Deep Sea Res.*, *37*, 809–832, doi:10.1016/0198-0149(90)90008-J.

Hansell, D. A., and C. A. Carlson (2001), Biogeochemistry of total organic carbon and nitrogen in the Sargasso Sea: Control by convective overturn, *Deep Sea Res., Part II*, *48*, 1649–1667, doi:10.1016/S0967-0645(00)00153-3.

Jenkins, W. J. (1977), Tritium-helium dating in the Sargasso Sea: A measurement of oxygen utilization rates, *Science*, *196*, 291–292, doi:10.1126/science.196.4287.291.

Jenkins, W. J. (1998), Studying tropical thermocline ventilation and circulation using tritium and 3He, *J. Geophys. Res.*, *103*, 15,817–15,831, doi:10.1029/98JC00141.

Jenkins, W. J., and S. C. Doney (2003), The subtropical nutrient spiral, *Global Biogeochem. Cycles*, *17*(4), 1110, doi:10.1029/2003GB002085.

Jenkins, W. J., and D. W. R. Wallace (1992), Tracer-based inferences of new primary production in the sea, in *Primary Productivity and Biogeochemical Cycles in the Sea*, edited by P. G. Falkowski and A. D. Woodhead, pp. 219–316, Plenum Press, New York.

Kadko, D. (2000), Modeling the evolution of the arctic mixed layer during the fall 1997 SHEBA project using measurements of ^{7}Be, *J. Geophys. Res.*, *105*, 3369–3378, doi:10.1029/1999JC900311.

Kadko, D., and R. Johnson (2008), Insights into 18 degree mode water formation from measurements of ^{7}Be at the Bermuda Time-series (BATS) station, paper presented at the Ocean Sciences meeting, Am. Soc. of Limnol. and Oceanogr., Orlando, Fla., 2–7 March.

Kadko, D., and D. Olson (1996), Be-7 as a tracer of surface water subduction and mixed layer history, *Deep Sea Res.*, *43*, 89–116, doi:10.1016/0967-0637(96)00011-8.

Kirchman, D. L., C. Lancelot, M. Fasham, L. Legendre, G. Radach, and M. Scott (1993), Dissolved organic matter in biogeochemical models of the ocean, in *Towards a Model of Biogeochemical Ocean Processes*, edited by G. T. Evans and M. J. R. Fusham, pp. 209–225, Springer, Berlin.

Krishnaswami, S., D. Lal, B. L. K. Somayajulu, F. S. Dixon, S. A. Stonecipher, and H. Craig (1972), Silicon, radium, thorium and lead in seawater: In-situ extraction by synthetic fibre, *Earth Planet. Sci. Lett.*, *16*, 84–90, doi:10.1016/0012-821X(72)90240-3.

Lal, D., Y. Chung, T. Platt, and T. Lee (1988), Twin cosmogenic radiotracer studies of phosphorus recycling and chemical fluxes in the upper ocean, *Limnol. Oceanogr.*, *336*, 1559–1567.

Lampitt, R. S., B. Boorman, L. Brown, M. Lucas, I. Salter, R. Sanders, K. Saw, S. Seeyave, S. J. Thomalla, and R. Turnewitsch (2008), Particle export from the euphotic zone: Estimates using a novel drifting sediment trap, ^{234}Th and new production, *Deep Sea Res., Part I*, *55*, 1484–1502, doi:10.1016/j.dsr.2008.07.002.

Lee, T., E. Barg, and D. Lal (1991), Studies of vertical mixing in the Southern California Bight with cosmogenic radionuclides ^{32}P and ^{7}Be, *Limnol. Oceanogr.*, *365*, 1044–1053.

Martin, J. H., G. A. Knauer, D. M. Karl, and W. W. Broenkow (1987), VERTEX: Carbon cycling in the northeast Pacific, *Deep Sea Res.*, *34*, 267–285, doi:10.1016/0198-0149(87)90086-0.

Martin, J. H., S. E. Fitzwater, R. M. Gordon, C. N. Hunter, and S. J. Tanner (1993), Iron, primary production and carbon-nitrogen flux studies during the JGOFS North Atlantic Bloom Experiment, *Deep Sea Res., Part I*, *40*, 115–134.

Martz, T. R., K. S. Johnson, and S. C. Riser (2008), Ocean metabolism observed with oxygen sensors on profiling floats in the South Pacific, *Limnol. Oceanogr.*, *53*, 2094–2111.

McGillicuddy, D. J., A. R. Robinson, D. A. Siegel, H. W. Jannasch, R. Johnson, T. D. Dickey, J. McNeil, A. F. Michaels, and A. H. Knap (1998), Influence of mesoscale eddies on new production in the Sargasso Sea, *Nature*, *394*, 263–265, doi:10.1038/28367.

Oschlies, A., and V. Garcon (1998), Eddy-induced enhancement of primary production in a model of the North Atlantic Ocean, *Nature*, *394*, 266–269, doi:10.1038/28373.

Sarmiento, J., G. Thiele, R. M. Key, and W. S. Moore (1990), Oxygen and nitrate new production and remineralization in the North Atlantic subtropical gyre, *J. Geophys. Res.*, *95*(C10), 18,303–18,315, doi:10.1029/JC095iC10p18303.

Silker, W. B. (1972), Beryllium-7 and fission products in the GEOSECS II water column and applications of their oceanic distributions, *Earth Planet. Sci. Lett.*, *16*, 131–137, doi:10.1016/0012-821X(72)90247-6.

Steinberg, D. K., S. A. Goldthwait, and D. A. Hansell (2000), Zooplankton vertical migration and the active transport of dissolved organic and inorganic carbon in the Sargasso Sea, *Deep Sea Res., Part I*, *47*, 137–158, doi:10.1016/S0967-0637(99)00052-7.

Williams, P. J. le B., and D. A. Purdie (1991), In vitro and in situ derived rates of gross production, net community production and respiration of oxygen in the oligotrophic subtropical gyre of the North Pacific Ocean, *Deep Sea Res.*, *38*, 891–910, doi:10.1016/0198-0149(91)90024-A.

Young, J. A., and W. B. Silker (1980), Aerosol deposition velocities on the Pacific and Atlantic oceans calculated from ^{7}Be measurements, *Earth Planet. Sci. Lett.*, *50*, 92–104, doi:10.1016/0012-821X(80)90121-1.

D. Kadko, RSMAS/MAC, University of Miami, 4600 Rickenbacker Causeway, Miami, FL 33140, USA. (dkadko@rsmas.miami.edu)